applied sciences

MDPI

Article

Influence of Polypropylene Fiber on Tensile Property of a Cement-Polymer Based Thin Spray-On Liner

Qun Wei [1,2], Nong Zhang [1,3,*], Xiaowei Feng [1], Zhengzheng Xie [1], Jiansheng Wu [2] and Juncai Cao [1,4]

1 Key Laboratory of Deep Coal Resource Mining, Ministry of Education of China, School of Mines, China University of Mining and Technology, Xuzhou 221116, China
2 Nanjing Branch of China Coal Technology and Engineering Group, Nanjing 210018, China
3 Jiangsu Normal University, Xuzhou 221116, China
4 ARC Centre of Excellence for Geotechnical Science and Engineering, Civil, Surveying and Environmental Engineering, The University of Newcastle, Callaghan, NSW 2308, Australia
* Correspondence: zhangnong@cumt.edu.cn

Received: 16 June 2019; Accepted: 16 July 2019; Published: 18 July 2019

Abstract: The influence of a polypropylene fiber on the tensile properties of a cement-polymer based thin spray-on liner (TSL) was investigated in this study. Two different contents of fiber were added to the liner, yielding two TSL groups. Tensile tests were performed (in accordance with the ASTM D638 standard) on the two groups of specimens as well as the control group at 1, 7, 14, and 28-day curing. The test result verified the large plasticity and low elastic modulus of the TSL compared with the fiber. SEM examination revealed that fibers lying parallel to the load direction ruptured or were pulled out from the matrix, which was beneficial to the tensile strength, but detrimental to the elongation because of their high stiffness. Other fibers lying perpendicular with the load direction were detrimental to both tensile strength and elongation through aggravating the propagation of the cracks. The tensile strength was improved by fiber incorporation, while the elongation was reduced at all curing. The influence of fibers on tensile toughness was uncertain since tensile toughness depended on strength as well as deformity.

Keywords: polypropylene fiber; tensile; cement polymer-based; thin spray-on liner; SEM

1. Introduction

1.1. Development of Thin Spray-On Liners

Thin spray-on liners (TSLs) are surface support materials that are sprayed onto the rock surface at a layer of 3 to 5 mm thickness [1]. TSLs (reactive or non-reactive) are generally cement, latex, and polymer-based. The first tests on TSLs were performed in Canada in the late 1980s. Initial research yielded a polyurethane-based product. Afterward, researchers from South Africa began exploring the use of a latex-based TSL [2]. As a sealant, TSLs can reduce weathering fretting, the permeability of shotcrete, and the corrosion of steel supports. Li [3] investigated, via experiments, the potential use of TSLs for gas management in underground coal mines. Observations from users have indicated that TSL support performance has, in most cases, exceeded expectations [4,5]. Guner [1] has summarized the following advantages of TSLs:

- Rapid curing rate and ability to reach adequate mechanical properties within a few hours after application;
- Low rebound amount and wastage during spraying process;
- Wide displacement range (elongation ratio);

- Ease and rapid rate of application;
- Smaller spraying equipment than that required for other liners;
- Less material handling with respect to other ground support products;
- Decrease in the operating costs;
- Lower thickness of applied material with respect to other surface support systems.

The mechanical performances of different TSLs have been determined worldwide, and of these the tensile performance is considered the most important. Nine support mechanisms have been summarized by Mpunzi, and at least six of these depend substantially or completely on the tensile strength contribution from the liner [4]. Hence, tension-related testing has been one of the most commonly employed physical property testing methods of thin spray-on liner (TSL) products worldwide. Tensile strength tests were conducted by Yilmaz and 21 TSL products were categorized on the basis of tensile strength [6]. A practical guide of a cement-based TSL was provided after the tensile creep behavior of this TSL was investigated by Guner [7]. The tensile toughness of TSL has been proposed as a new performance criterion for TSL, and various TSL energy absorption capacity values were determined [1].

1.2. Support Provided by TSLs

A TSL is chemically bonded to the rock surface, allowing for early mobilization of the support, thereby serving as a complement to reinforcement that helps the rockmass to support itself [8]. Compared with other surface support, such as mesh, TSLs can offer support resistance at small displacement, and can therefore prevent the occurrence of rockfalls [2]. The support effectiveness of TSLs has been evaluated in several studies.

Experiments by Shan et al. indicated that the bonding characteristics of a TSL material yields a composite layer with the rock skin, thereby increasing the specimen resistance to rock skin failure [9]. The results of a large-scale guttering test indicated that a TSL is better than steel mesh in restricting rock movement and thus inhibiting the formation of gutters in the roof [10]. Field-scale explosive detonations have been conducted in other work [11]. The findings validated that TSLs and variant layer combinations may be as effective or superior to conventional support materials for mitigating rockburst or similar damage in highly stressed mine environments. Due to its benefits, TSL has attracted increasing attention as an alternative to steel mesh in underground roadway support [12–15]. These liners may be used in hard rock mines and coal mines [2,16–18].

1.3. Fiber-Reinforced Materials and Fiber-Reinforced TSLs

Fibers has been widely used to improve concrete properties, of which plastic fibers are of great advantages. According to Joong [19], tunneling shotcrete with 0.6–0.8% volume content of polyamide-fiber-reinforced shotcrete can yield significant improvement in the flexural ductility, toughness, and ultimate load capacity. Cheng [20] reported that fiber addition prevents the formation of plastic shrinkage cracks in underground shotcrete. Yin [21] reviewed that plastic fibers are synthetic fibers, which can be in the form of micro plastic fibers(with the diameter of 5 to 100 μm and length of 5–30 mm) or macro plastic fibers (which have a length of 30–60 mm and cross section of 0.6–1 mm^2). Polypropylene, polyester, and high density polyethylene (PP, PET, and HDPE) are the three main raw materials used in the production of plastic fibers, and polypropylene fibers have become the most common commercial products in fiber-reinforced concrete. Liu [22] use polypropylene fiber as well as organic polymer to reinforce sand and concluded that through the interaction force among fibers and sand particles and the bonding force of polymer among sand particles, tensile strength of reinforced sand is greatly improved.

Published studies on fiber-reinforced TSLs are rare. Resin-based TSLs with glass fiber (placed in several layers in the specimens) have been investigated by Shan [8]. The results revealed that the tensile and flexural strengths of the polymers increased, owing to the fiber addition. Qiao [23] investigated cube samples containing glass fiber, and the results indicated that samples with fiber are stronger than those without fiber. In another study [24], the shear strength of the polymer material was significantly improved, owing to the addition (layer-wise) of glass fiber, which is beneficial for supports in underground mines. Cement-polymer based TSLs always behaved lower tensile performances compared with the resin-based ones in the aforementioned three tests. The tensile strength of cement-polymer TSLs were much lower than that of polyurethane at a 4 mm thickness [2]. However, many of the rock support mechanisms provided by sprayed liners depend substantially or completely on the tensile strength contribution of the liner [4]. Therefore, the improvement of tensile performance is of great necessity.

A TSL is usually sprayed onto the rock substrate. Fiber with a small length and diameter may be of ease to be pumped and conveyed. Consequently, microfibers such as PP are preferred for TSL reinforcement in the perspective of application. In this study, the influence of fiber addition on the tensile performance of TSL samples was investigated by adding two different contents of polypropylene fiber to a cement-polymer based TSL product. Control samples were also investigated. Samples with different fiber content were tested at separate curing times of 1, 7, 14, and 28 days.

2. Material and Methods

2.1. Cementitious Polymer and Polypropylene Fibers

The tests were conducted with a TSL product in the powder state. This powder is based on cementitious polymer-modified systems that undergo curing mainly via water loss from the polymer emulsion, thereby allowing the polymer film to form and gain strength. The TSL product and company name are excluded from this study due to confidentiality. The polypropylene fiber employed in this test is commonly utilized for concrete reinforcement in construction engineering (see Table 1 and Figure 1 for the mechanical properties and a SEM image, respectively, of the fiber).

Table 1. Physical properties of polypropylene fiber utilized.

Diameter (µm)	Average Length (mm)	Tensile Strength (MPa)
18–80	3	>458

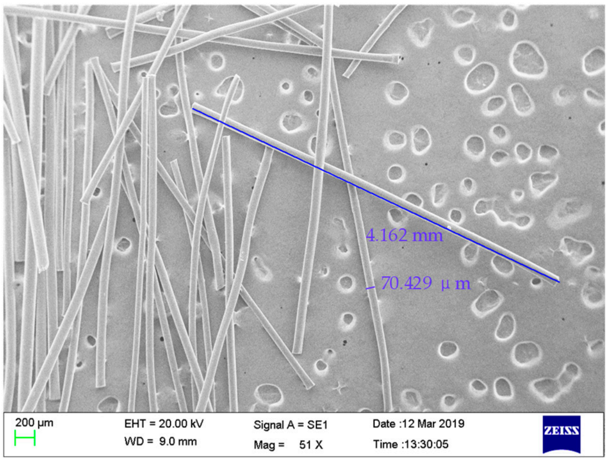

Figure 1. Polypropylene fiber used in this study.

Two different contents of polypropylene fiber were added, yielding two different groups referred to as TF-A (Thin spray-on liner with Fiber, fiber content A) and TF-B, with fiber dosages of 1%, and 2% by weight, respectively. The control group (i.e., plain TSL) was referred to as PT (Plain Thin spray-on liner). Water-powder ratios of 0.4–0.6 by weight were recommended by the operation instructions of the TSL manufacturer. The laboratory test showed that the mixture sets within a few minutes. Hence, to maintain the fluidity of the slurry prior to its consolidation, a maximum water-powder ratio of 0.6 was adopted for all four groups of specimens.

2.2. Sample Preparation

A molding method has been widely employed in the tensile testing of TSLs. However, shrinkage of specimens in the dogbone mold was considerable at long curing periods (7 days and longer). The specimen dimensions decreased significantly, resulting in non-conformity with the D638 standard. Die cutting has been recommended as an alternative method. However, use of this method revealed that the edges of samples could be easily destroyed during the die cutting process of 1-day specimens. This resulted mainly from inadequate overall strength of the samples. Both methods were employed in the present study. The molding method was adopted for the 1-day curing period samples, while 7, 14, and 28-day curing samples were prepared via the die cutting method.

All samples of a group were prepared in exactly the same manner. For curing periods longer than 7 days, specimens of different groups were die cut from separate TSL sheets. A kitchen mixer was used and the same rotational speed and mixing time were adopted for all the groups. The mixture was vacuumed for 2 min, accompanied by vibrating on a table vibrator, prior to pouring, to expel air bubbles. Fiber-containing mixtures were obtained by adding fibers to water at first and mixing with the mixer for 1 min, ahead of the mixing with powder. The same process of vacuuming and vibrating was adopted for the fiber-containing mixtures as well. Specimens were demolded (for 1-day curing) or die cut (for 7, 14, and 28-day curing) immediately preceding test execution. See Figure 2.

The dogbone mold was fabricated from a 5-mm-thick PMMA sheet. A plastic plate with four bars forming a rectangular space was used to mold the TSL sheets for die cutting. A wooden base cutter was used, with a blade embedded in a plank, as shown in Figure 2d. An electric mixer for kitchen use and a table vibrator (frequency: 2860 per min, amplitude: 0.3–0.6 mm) were employed. To facilitate demolding, oil films were brushed onto the dogbone mold and plastic plate. All the specimens were prepared on the same day and cured together to maintain the uniformity.

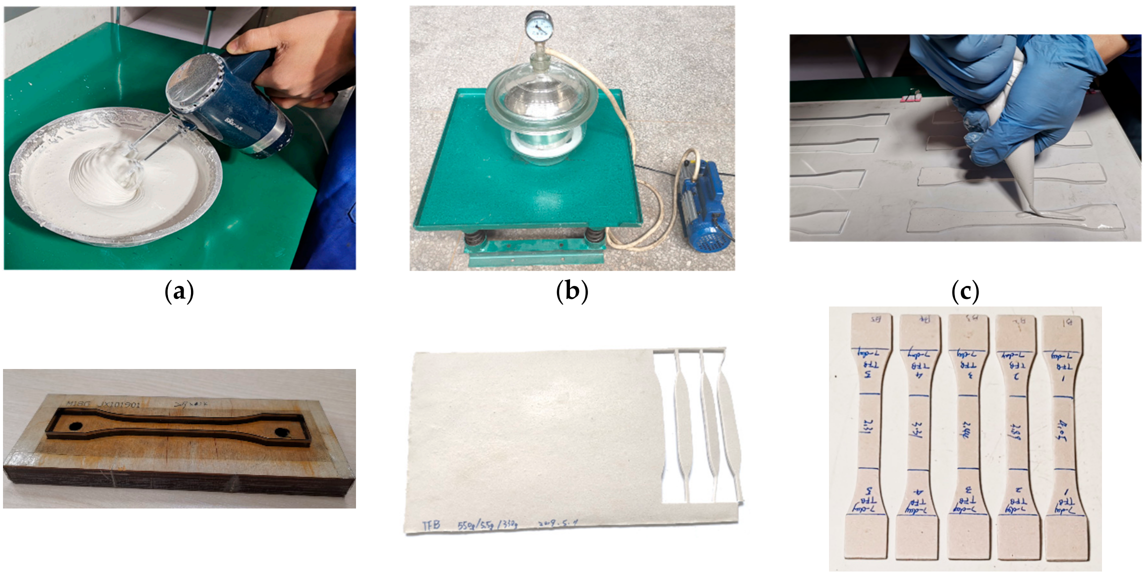

(**a**) (**b**) (**c**)

(**d**) (**e**) (**f**)

Figure 2. Specimen preparation. (**a**) mixing with a kitchen mixer, (**b**) vibrating and vacuuming, (**c**) dogbone molding, (**d**) die cutter, (**e**) sheet for die cutting, (**f**) specimens by die cutting.

2.3. Viscosity

A rotary viscometer was used to measure the viscosity of the slurry with different fiber addition. Test was executed after the water, powder and fiber (for TF-A and TF-B) was mixed for 60 s. The No. 4 rotor with a rotation speed of 12 r/min was adopted, producing a measuring range 50,000 mPa·s. The test result was shown in Figure 3.

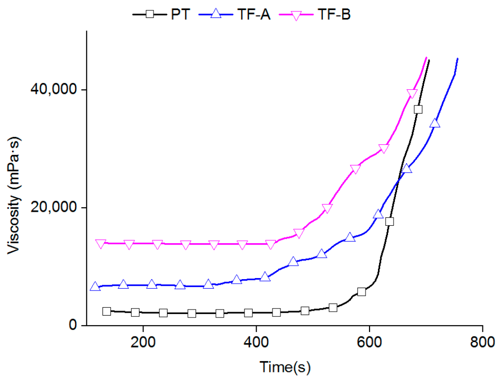

Figure 3. Viscosity of the three kinds of slurry.

Viscosity of the PT slurry increased rapidly after keeping steady for about 10 min. Slurry with fiber exhibited a relatively higher viscosity during the steady period, prior to increasing at much earlier time than that of the PT slurry. The addition of fiber increased the viscosity of the TSL slurry distinctly, which may be detrimental to the bubble expelling and therefore the integrity of the specimens.

2.4. Water Loss

Water loss process was monitored during the specimens curing. 3 bars with a dimension of 150 mm × 20 mm were cut respectively from the 3 sheets of different fiber dosage for die cutting respectively, after the sheets was cured for 1 day. A high-accuracy electronic scale was used to measure the weight change of the bars. The electric scale and bars were shown in Figure 4. Relative weight during different curing was achieved by dividing the measured weight by its original value. As shown in Figure 5, water loss was significant at the early curing especially during the first day of monitoring. Weight of the bars dropped slowly from 2–10 curing days and remained stable after 10-day curing. Relative weight of PT, TF-A and TF-B were 0.840, 0.845, and 0.859 at 7-day curing, and the corresponding value were 0.830, 0.836 and 0.850 at 28-day curing, showing little difference between different groups at a same curing period. Consequently, fiber addition might have little influence on the tensile strength through changing the water loss rate at different curing.

(**a**) (**b**)

Figure 4. Water loss monitoring. (**a**) high-accuracy electronic scale, (**b**) bars for weighting.

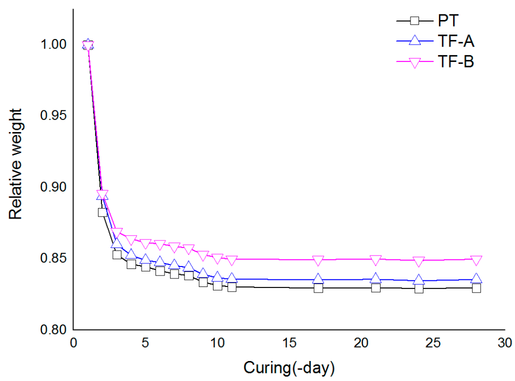

Figure 5. Relative weight changing during curing.

2.5. *Tensile Strength, Elongation at Break and Tensile Toughness*

ASTM D638 standard is the most widely used testing method adopted by researchers in practice [1,5,25,26], and is recommended by EFNARC (European Federation of National Associations Representing producers and applicators of specialist building products for Concrete) for tensile test of TSLs [27]. In the present study, tensile tests were performed in accordance with this standard. The Type I specimen shape (dogbone or dumbbell shape) stipulated in the D638 standard was adopted, as shown in Figure 6.

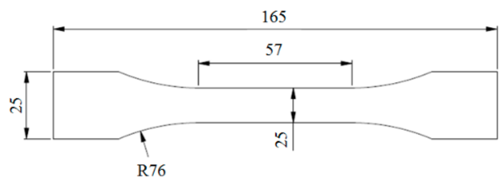

Figure 6. Specimen shapes and dimensions (mm) in accordance with ASTM D638.

The tensile strength of each specimen was calculated from Equation (1).

$$S\_t = l\_p/(W \times T), \tag{1}$$

where l_p is load (N) at failure, W (mm) is width of the specimen and T (mm) is thickness of the specimens.

Since the gauge length is 50 mm, the elongation at break is calculated by dividing the deform value (in mm) at break by 50.

Toughness is defined as the capacity of a material to absorb energy prior to fracturing. This parameter is generally referred to as tensile toughness or the modulus of toughness and described by U_t. The toughness can be calculated as the whole area under the stress-strain curve, and calculated as [1]:

$$U_t = \int_0^{\varepsilon_f} \sigma d\varepsilon, \tag{2}$$

where ε_f is the strain at fracture.

2.6. *SEM Analysis*

Scanning electron microscopy (SEM) is an indispensable tool for exploring the micro-world and characterizing the surface structure and composition in scientific research and industrial production. SEM was employed in this study for the visible examination. Particularly, the Quanta 250 SEM (FEI, Brno, Chech) equipment was employed for the observation of the fracture surface.

3. Test Setup and Execution

The tests were performed on a material testing machine (the test setup is shown in Figure 7). A data acquisition system with a data reading capability of 10 Hz was used. The tensile load was measured by an S-type load cell with a 1000 N capacity, and the deform value was recorded by the extensometer. Depending on the specification of the material being tested, the D638 standard suggests different testing speeds, which will generate rupture within 0.5–5 min of testing. However, elongations at different curing periods varied considerably. A 10 mm/min loading rate was employed, and changes in the displacement of the grips were measured by the extensometer. The gauge length was set to be 50 mm according to the D638 standard. A total of 80 specimens were tested.

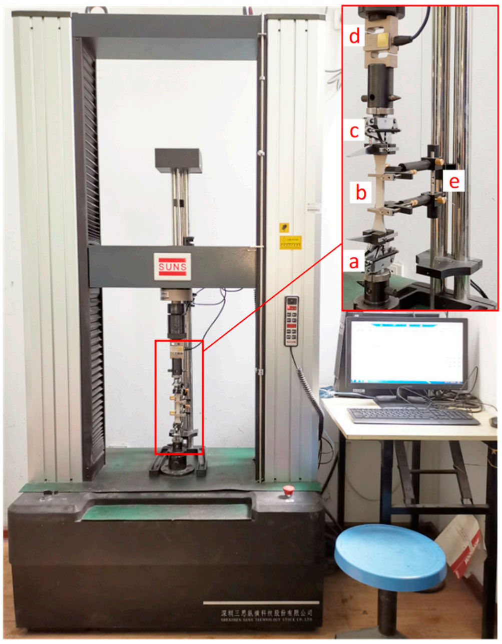

Figure 7. Test setup. (**a**) lower grip, (**b**) specimen, (**c**) upper grip, (**d**) load cell, (**e**) extensometer.

Most of the specimens ruptured in the gauge length, as shown in Figure 8a. These specimens are valid ones according to the test standard. However, several specimens ruptured out of the gauge length. See Figure 8b. Such specimens were eliminated for test result calculation. Macroscopic fibers were observed at the fracture surface of the fiber-containing specimens, see Figure 8c.

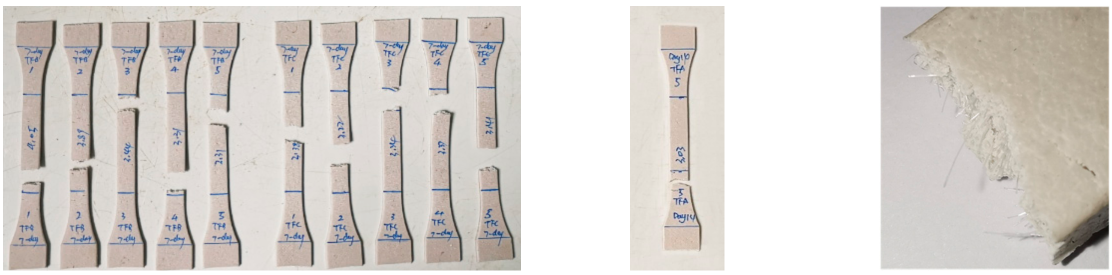

(**a**) (**b**) (**c**)

Figure 8. Specimens after rupture and the occurrence of fracture. (**a**) specimens ruptured in the gauge length, (**b**) a specimen ruptured out of the gauge length, (**c**) fracture surface of a fiber-containing specimen.

4. Test Results and Discussions

4.1. Stress-Strain Curve

Relationships between stress and strain based on averaged data of valid specimens associated with different curing periods are shown in Figure 9.

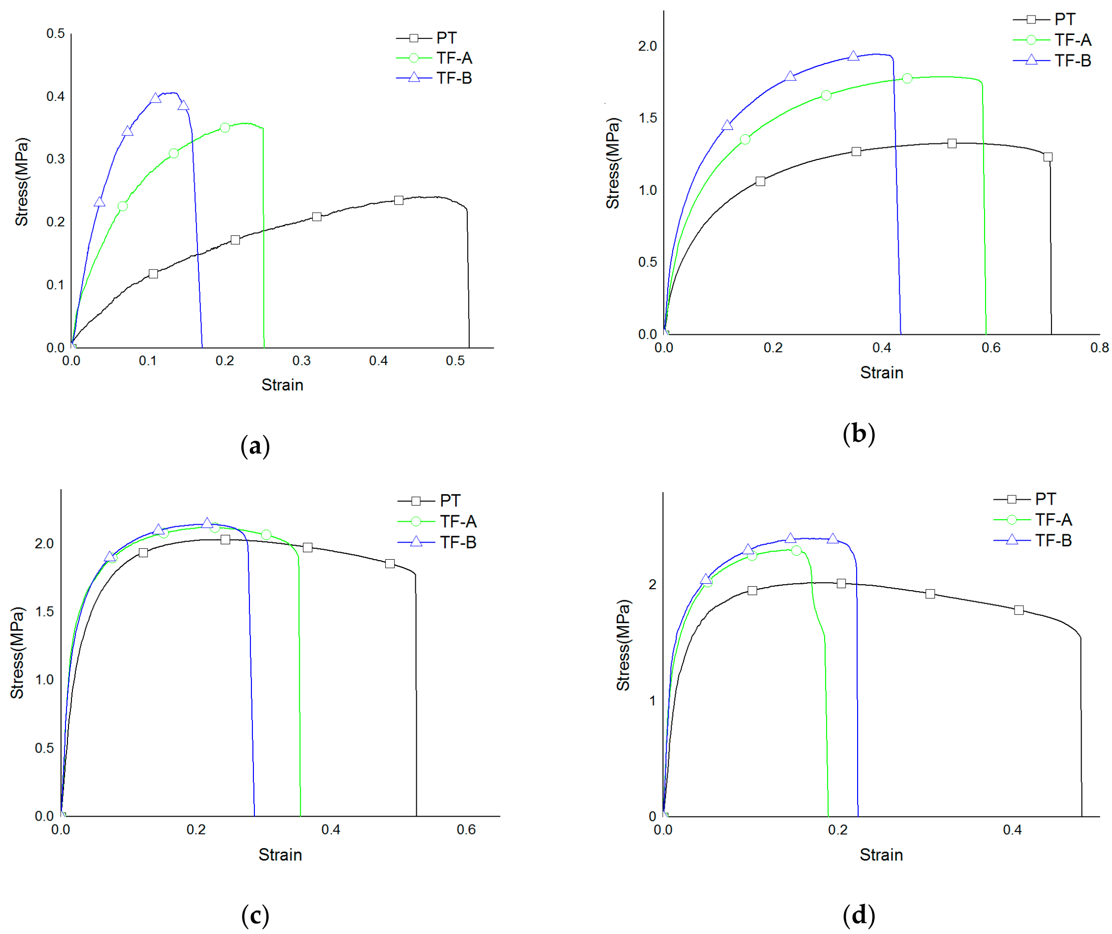

Figure 9. Stress versus strain relationship associated with different curing times of typical specimens. (**a**) 1-day curing, (**b**) 7-day curing, (**c**) 14-day curing, (**d**) 28-day curing.

As shown in Figure 9, the stress values increased at distinctly different rates during 1-day curing of the four different groups. The stress of TF-A and TF-B increased considerably more rapidly than that of PT during 1-day curing, giving rise to an "n" type curve in each case. In contrast, "L" type curves were obtained for groups PT. Meanwhile specimens ruptured rapidly after peak stress during 1-day curing. Such disparities receded at 7-day curing. However, at 14-day and 28-day curing, the stress associated with specimens of different groups increased at similar rates. In particular, the strength of the specimens at 1-day curing was extremely low and, hence, the corresponding curves exhibited significant fluctuation after peak load at 1-day curing. Additionally, specimens at long curing yielded a big deformation after peak stress.

All the groups exhibited a very short elastic period at the beginning, especially at long curing. The elasticity modulus of TF-B at 28-day curing, being the highest one of all, was 149.82 MPa. It is much smaller than that of the PP fiber employed in the test. In contrast, all the groups exhibited obvious plasticity, particularly at 14-day and 28-day curing. The elasticity and plasticity of the tested TSL differed greatly from the employed PP fiber.

4.2. Tensile Strength

The average tensile strength was determined by the valid specimens. The mean values as well as standard deviation associated with different fiber contents and different curing periods are listed in Table 2.

Table 2. Tensile strength at different curing periods (MPa).

Group	1-Day	7-Day	14-Day	28-Day
PT	0.24 ± 0.008	1.33 ± 0.155	1.98 ± 0.030	2.04 ± 0.026
TF-A	0.37 ± 0.018	1.80 ± 0.110	2.12 ± 0.033	2.34 ± 0.049
TF-B	0.41 ± 0.028	1.95 ± 0.066	2.15 ± 0.091	2.44 ± 0.077

As shown in Table 2, fiber incorporation resulted reinforcement to the tensile strength of specimens at all curing periods. Moreover, specimens with 2% fiber addition exhibited higher tensile strength than that of 1% fiber addition at the same curing period.

Figure 10 shows the relationship between the tensile strength and curing time of each group. As shown in the figure, the strength depended strongly on time. For all three groups, the tensile strength increased rapidly during the 1-day to 7-day curing period, then after the 7-day period, showing a similar tendency with that of water loss.

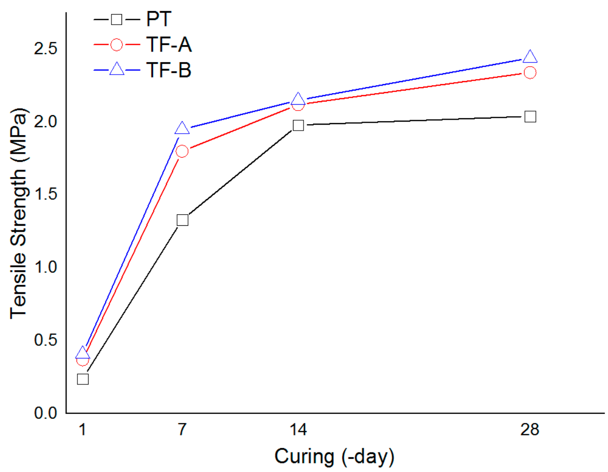

Figure 10. Relationship between average tensile strength and curing period.

4.3. Elongation

Deformability plays a more significant role in the performance of TSL than in the performance of other liners such as shotcrete. The comparison of average values with error bars of valid specimens is shown in Figure 11.

For both groups at all curing periods, the addition of fiber resulted in decreased elongation at break and the value varied with the dosage. This may have resulted from the fact that the stiffness of the fiber is higher than that of the TSL specimen. The aforementioned decrease was considerable at early curing times of 1 day. At 1-day curing, the average value of TF-A and TF-B was only 55%, and 32% of that corresponding to plain TSL. The addition of fiber is detrimental to the deformability of the TSL.

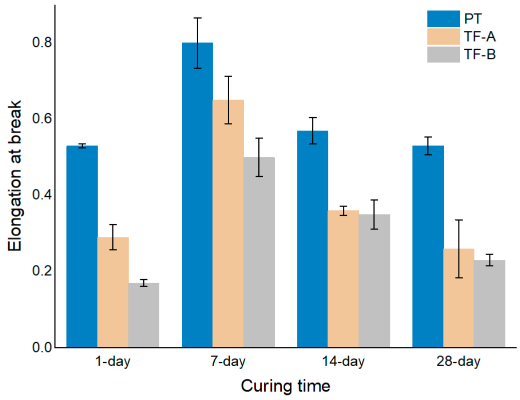

Figure 11. Comparison of elongation at break.

4.4. Tensile Toughness

The average values of tensile toughness with error bars at different curing are compared in Figure 12.

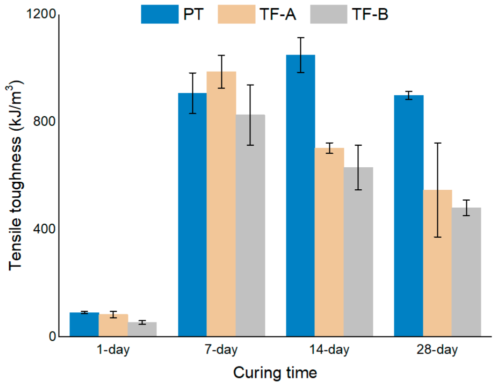

Figure 12. Comparison of tensile toughness at different curing.

Curing period showed great impact on the tensile toughness. All the three groups exhibited a very weak tensile toughness at 1-day curing which might result from the low tensile strength. The tensile toughness improved distinctly from 1-day to 7-day curing. For PT group, it exhibited a best tensile toughness at 14-day curing, which was in accordance with its performance of elongation. The curing time exerted considerably more influence on the tensile toughness of fiber-contained groups than of the PT groups. Tensile toughness of the fiber-contained groups decreased distinctly from 7-day to 28-day curing, behaving in a same way as the elongation. At long curing periods (14 and 28-day), the addition of fiber exerted considerably more influence on the tensile toughness. The higher fiber dosage resulted in a lower tensile toughness.

4.5. SEM Analysis and Discussion

A scanning electron micrograph of the fracture surface corresponding to a 28-day curing TF-A specimen is shown in Figure 13. Porosities of different diameters occurred on this surface and may have resulted from the following factors: the remaining tiny bubbles, which were probably generated during mixing of the slurry containing the TSL powder and water. The slurry exhibited high viscosity and easily lost fluidity. Therefore, the elimination of bubbles via vacuuming and vibrating was difficult. A cement-polymer based TSL powder was considered, and the loss of water from the specimens during curing may have also contributed to the occurrence of the aforementioned porosities. Porosities is potentially detrimental to the integrity therefore the tensile performance of the TSL. As shown in

Figure 4, slurries with fiber exhibited a higher viscosity than that of plain TSL. Thus, fiber addition is potentially detrimental to the tensile performances from the perspective of improved viscosity.

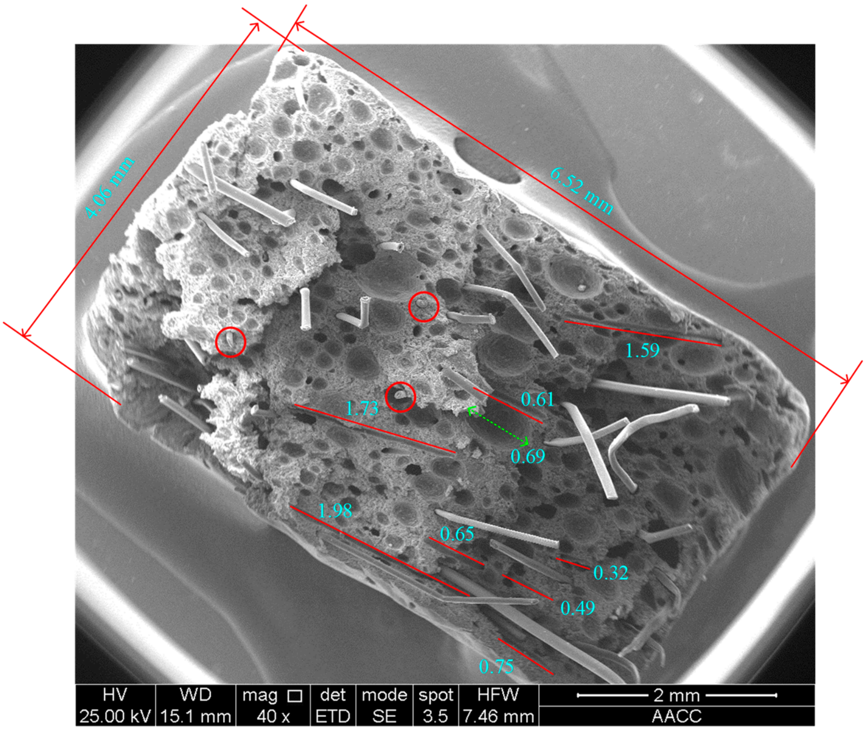

Figure 13. Scanning electron micrograph of a fracture surface.

Fibers in the TSL matrix were lying in random orientation. As shown in Figure 9, rare (only three that were recognized) fibers were broken exactly at the fracture surface of the specimen (see circled regions in Figure 13). Tens of the fibers in the SEM picture seemed to be pulled out from the substrate and this can also be observed in Figure 8c. This phenomenon may owe to the huge difference of the elasticity and plasticity between the PP fibers and the TSL matrix. However, fibers played a role of bridging the matrix at the fracture surface before they were broken or pulled out from the matrix. Thus, fibers lying parallel with the loading direction were beneficial to the tensile strength of the specimen.

The pulled out fibers indicated the poor adhesion between the fiber and the matrix. Strong adhesion will absolutely improve the tensile strength owing to the higher stiffness of fibers than that of the TSL matrix. Choi [28] carried out some experiments on the influence of silicone oil on load-reducing fiber-reinforced polymer cement mortar. They observed from SEM that the fibers were pulled out while maintaining its shape as the adhesion between the fiber and matrix was degraded due to the silicone oil. They argued that the reduction in adhesion between the fiber and the matrix had an impact (reduction) on the strength characteristics. However, additional investigation on the influence of adhesion between fibers and matrix on tensile strength of fiber-reinforced materials is needed.

On the other hand, there were an amount of fibers that lay fully or partly in the fracture surface. The evidence was the straight openings of different length that can be seen notably at the fracture face, which were marked with red lines (with the length of each other nearby) in Figure 13. Failure process of plain TSL is illustrated in Figure 14. Tiny cracks began to occur when the specimen was loaded Figure 14a. With the growing of load, more cracks were generated and the cracks propagated Figure 14b. The propagated cracks connected with the adjacent ones and finally made the rupture of the specimen Figure 14c. Concerning to the fiber contained specimens, fibers lying perpendicular with the loading direction undoubtedly aggravated the propagation of the cracks and therefore the rupture of the specimens. Hence, specimens with fibers exhibited a quite smaller elongation at rupture than that of plain TSL, and fiber incorporation is detrimental to the deformability of the TSL. Such perpendicular fibers were detrimental to the tensile strength, however, this reduction might be overcome by the benefit of the parallel ones in this test.

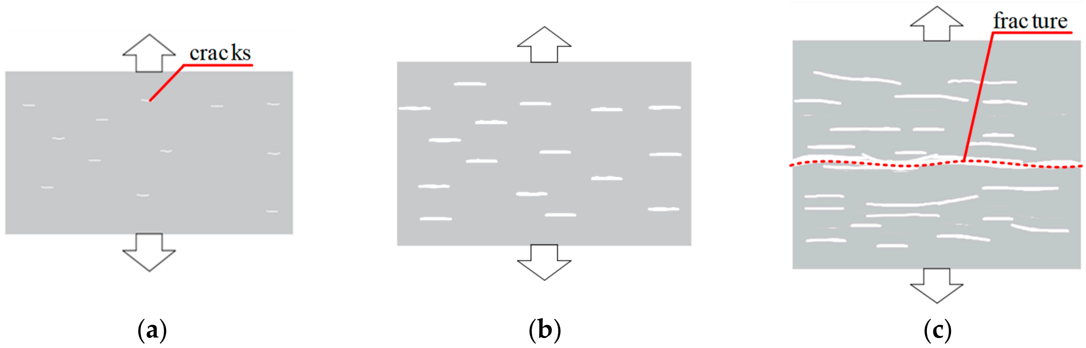

Figure 14. Failure process of plain TSL. (**a**) Tiny cracks occurred, (**b**) cracks propagated, (**c**) rupture occurred.

Since the tensile toughness depends on both the stress and deformability, the influence of fibers on tensile toughness were indeterminate for the influence of fiber on the tensile strength and elongation is not coincident. The influence on tensile strength and elongation varied notably at different curing periods. Consequently, the comparison of tensile toughness varied at different curing. TF-A group exhibited a higher tensile toughness at 1-day curing than the other groups, probably resulting from its higher tensile strength (compared with PT) and higher elongation (compared with TF-B). However, fiber incorporation improved the tensile strength tightly, while reducing the elongation heavily at 14 and 28-day curing. Consequently, specimens at these curing periods exhibited a quite weaker tensile toughness. Overall, the influence of fiber on tensile performances of TSL is quite uncertain.

5. Conclusions

The addition of polypropylene fiber increased the viscosity of the cement-polymer based TSL slurry distinctly in this study, which may be detrimental to the bubble expelling and therefore the integrity of the specimens. The influence of fiber addition was insignificant on water loss. Consequently, fiber addition could not affect the tensile strength through changing the water loss rate. Examination from the SEM showed that most fibers lying parallel to the loading direction might be pulled out from the matrix or break at the fracture surface, which was beneficial to the tensile strength because of the high stiffness of the fibers. In contrast, these fibers reduced the deformation and were detrimental to the elongation. Meanwhile, an amount of fibers was fully or partly in the fracture surface (that is perpendicular with the load direction), aggravating the propagating of the cracks therefore reducing the elongation at break as well as the tensile strength of the specimens. The cementitious polymer TSL tested in this study was of obvious plasticity judging from the stress-strain curves. The influences of PP fiber varied on different tensile performances of the TSL. With respect to the tensile strength, the enhancement might be dominating, thus the tensile strength was improved at all curing periods by fibers. In contrast, fibers were completely detrimental to the elongation at all curing periods. The influence of fibers on tensile toughness was uncertain at different curing periods, for it was determined by both the stress and deformity of the specimens.

Author Contributions: All of the authors contributed extensively to the work. Q.W., N.Z. proposed key ideas. Q.W., J.W. conceived and designed the experiment schemes. Q.W. conducted the experiment. Q.W. and Z.X. analyzed the data. Q.W. wrote the paper. X.F. and J.C. modified the manuscript.

Funding: This research was funded by the Fundamental Research Funds for the Central Universities (2017CXNL01).

Acknowledgments: We thank Liwen Bianji, Edanz Editing China (www.liwenbianji.cn/ac), for editing the English text of a draft of this manuscript.

Conflicts of Interest: The authors declare no conflict of interest.

References

1. Guner, D.; Ozturk, H. New performance criterion for thin spray-on liners tensile toughness. In Proceedings of the 50th US Rock Mechanics/Geomechanics Symposium, American Rock Mechanics Association, Houston, TX, USA, 26–29 June 2016.
2. Tannant, D.D. Thin spray-on liners for underground rock support. In Proceedings of the 17th International Mining Congress and Exhibition of Turkey (IMCET 2001), Ankara, Turkey, 19–22 June 2001.
3. Li, Z.; Hussain, F.; Mitra, R.; Saydam, S. Effectiveness of thin spray-on liners as a gas management tool in underground coal mines. *Int. J. Coal. Geol.* **2016**, *168 Pt 2*, 193–201. [CrossRef]
4. Mpunzi, P.; Masethe, R.; Rizwan, M.; Stacey, T.R. Enhancement of the tensile strengths of rock and shotcrete by thin spray-on liners. *Tunn. Undergr. Space Technol.* **2015**, *49*, 369–375. [CrossRef]
5. Jjuuko, S. A review of application and benefits of thin spray-on liners for underground rock support in South African mines. In Proceedings of the 8th South African Young Geotechnical Engineers Conference, Western Cape, South Africa, 17–19 September 2014.
6. Yilmaz, H. Tensile strength testing of thin spray-on liner products (TSLs) and shotcrete. *J. South. Afr. Inst. Min. Metall.* **2010**, *110*, 559–569.
7. Guner, D.; Ozturk, H. Creep behaviour investigation of a thin spray-on liner. *Int. J. Rock Mech. Min. Sci.* **2018**, *108*, 58–66. [CrossRef]
8. Potvin, Y.; Stacey, T.R.; Hadjigeorgiou, J.; Yilmaz, H. *Surface Support in Mining*; Australian Centre for Geomechanics: Perth, Australia, 2004.
9. Shan, Z.; Porter, I.; Nemcik, J.; Baafi, E. Investigating the behaviour of fibre reinforced polymers and steel mesh when supporting coal mine roof strata subject to buckling. *Rock Mech. Rock Eng.* **2018**, *52*, 1–13. [CrossRef]
10. Shan, Z.; Porter, I.; Nemcik, J.; Baafi, E. Comparing the reinforcement capacity of welded steel mesh and a thin spray-on liner using large scale laboratory tests. *Int. J. Min. Sci. Technol.* **2014**, *24*, 373–377.
11. Archibald, J.F.; Dirige, P.A. Development of thin, spray-on liner and composite superliner area supports for damage mitigation in blast- and rockburst-induced rock failure events. *WIT Trans. Built Environ.* **2006**, *87*, 237–246.
12. Ozturk, H. Fracture mechanics interpretation of thin spray-on liner adhesion tests. *Int. J. Adhes. Adhes.* **2012**, *34*, 17–23. [CrossRef]
13. Ozturk, H. Work of adhesion of thin spray-on liners. *Rock Mech. Rock Eng.* **2012**, *45*, 1095–1102. [CrossRef]
14. Tibbs, M.P.; Tyler, O.K.; Van Duin, S.; Baafi, E. Autonomous thin spray-on liner application in irregular tunnel and mine roadway surfaces. In Proceedings of the 30th International Symposium on Automation and Robotics in Construction and Mining, Montreal, QC, Canada, 11–15 August 2013.
15. Qiao, Q.; Nemcik, J.; Porter, I.; Baafi, E. Laboratory tests on thin spray-on liner penetrated rock joints in direct shear. *Rock Mech. Rock. Eng.* **2015**, *48*, 2173–2177. [CrossRef]
16. Li, Z.; Saydam, S.; Mitra, R.; Chalmers, D. Investigation on adhesion strength of thin spray-on liners in an underground coal mine. In Proceedings of the 15th Coal Operators' Conference, University of Wollongong, The Australasian Institute of Mining and Metallurgy, Mine Managers Association of Australia, University of Wollongong, NSW, Australia, 11–13 January 2015.
17. Ferreira, P.H.; Piroddi, A. The application of GRP and thin spray liner support products in a typical block cave mining method to enhance safety and productivity. In Proceedings of the 6th Southern African Base Metals Conference 2011, Phalaborwa, South Africa, 18–20 July 2011.
18. Komurlu, E.; Kesimal, A. Usability of thin spray-on liners (TSL) for akarsen underground mine in Murgul. In Proceedings of the 25th International Mining Congress and Exhibition of Turkey, Antalya, Turkey, 11–14 April 2017.
19. Jeon, J.K.; Kim, W.; Kim, G.Y.; Jeon, C.K. Polyamide fiber reinforced shotcrete for tunnel application. *Materials* **2016**, *9*, 163. [CrossRef] [PubMed]
20. Cheng, W.; Liu, G.; Chen, L. Pet fiber reinforced wet-mix shotcrete with walnut shell as replaced aggregate. *Appl. Sci.* **2017**, *7*, 345. [CrossRef]
21. Yin, S.; Tuladhar, R.; Shi, F.; Combe, M.; Collister, T.; Sivakugan, N. Use of macro plastic fibres in concrete: A review. *Constr. Build. Mater.* **2015**, *93*, 180–188. [CrossRef]

22. Liu, J.; Chen, Z.; Song, Z.; Bai, Y.; Qian, W.; Wei, J.; Kanungo, D.P. Tensile behavior of polyurethane organic polymer and polypropylene fiber-reinforced sand. *Polymers* **2018**, *10*, 499. [CrossRef] [PubMed]
23. Qiao, Q.; Nemcik, J.; Porter, I.; Baafi, E. Compressive strength testing of Toughskin thin spray-on liner. In Proceedings of the 15th Coal Operators' Conference, University of Wollongong, The Australasian Institute of Mining and Metallurgy, Mine Managers Association of Australia, University of Wollongong, NSW, Australia, 11–13 January 2015; pp. 198–203.
24. Qiao, Q.; Nemcik, J.; Porter, I. Shear strength testing of glass fibre reinforced thin spray-on liner. *Géotech. Lett.* **2014**, *4*, 250–254. [CrossRef]
25. Guner, D.; Ozturk, H. Experimental and numerical analysis of the effects of curing time on tensile mechanical properties of thin spray-on liners. *Rock Mech. Rock Eng.* **2016**, *49*, 3205–3222. [CrossRef]
26. Guner, D.; Ozturk, H. Tensile-creep test specimen preparation practices of surface support liners. *IOP Conf. Ser. Earth Environ. Sci.* **2017**, *95*, 42004. [CrossRef]
27. EFNARC. *Specification and Guidelines on Thin Spray-on Liners for Mining and Tunnelling*; ENC 250TSL v7.2 25–07–08; EFNARC: 2008.
28. Choi, H.; Choi, H.; Lee, B.; Lee, D. Shrinkage and durability evaluation of environmental load-reducing FRPCM by using silicone oil. *Materials* **2019**, *12*, 1240. [CrossRef] [PubMed]